

SEISMIC BEHAVIOR OF MULTI-SPAN GIRDER BRIDGES FOR SPATIALLY VARYING RANDOM GROUND MOTIONS INCLUDING FOUNDATION INTERACTION

El--Sayed Amin Mashaly

Structural Engineering Department, Faculty of Engineering,
Alexandria University, Alexandria, Egypt.

ABSTRACT

The seismic behavior of multi-span girder bridges to spatially varying random ground motions including the foundation interaction is studied. The seismic excitation is represented by the three translational components of earthquake ground motions acting at the bridge supports. These motions are idealized as stationary or nonstationary partially correlated random processes characterized by Power Spectral Density (PSD), Evolutionary Spectral Density (ESD) or double frequency Generalized Spectral Density (GSD) functions. The soil-structure interaction for rectangular supports of the bridge is represented by frequency-dependent impedance functions which are expressed by empirical formulas representing both the stiffness and damping of soil. For stationary seismic excitation, spectral analysis is carried out in the frequency domain to obtain the spectral moments of response from which the root mean square (r.m.s) and peak responses are evaluated. For nonstationary seismic excitation, both evolutionary and generalized double frequency stochastic analyses are conducted to obtain the time-dependent r.m.s and peak responses. The evolutionary spectral analysis facilitates the computations through a reduction in the multiplicity of the integrals involved in the double frequency generalized spectral analysis for the evaluation of the response covariance matrices. A parametric study is made to specifically investigate the seismic behavior of multi-span girder bridges and the influence of some factors on their responses. The following four items are of particular importance: (i) the characteristics of multiple support excitations, such as the nonstationarity, duration, cross correlation and direction of seismic waves, (ii) the soil-support interaction with variable embedment depth and shape ratio of supports, (iii) the variation of dynamic properties of the near field soil, and (iv) the stiffness and length of the bridge (with or without flexible joints). The numerical results indicate that: (a) the time-dependent mean peak internal forces increase with the increase of earthquake duration, but do not overshoot the corresponding stationary values, (b) for a realistic evaluation of seismic stresses induced in the different sections of the bridge, the spatial variation of multiple support excitation has to be considered, (c) minimum internal forces are produced if the bridge is oriented perpendicular to the direction of wave propagation, (d) if the bridge is supported on soft soil, the soil-support interaction results in a significant reduction of stresses, (e) the internal forces are minimized for surface square supports, and (f) more flexible joints are recommended to be imposed near the interior supports to overcome the enhancement of bending moments.

Keywords: *Structural engineering, Dynamics, Earthquake engineering.*

INTRODUCTION

During many major earthquakes, serious damages to multi-span bridges have been reported. Damage of

bridge may lead to loss of vital services and transportation systems. Therefore, a realistic

evaluation of stresses induced by seismic excitation at different sections of bridge is important. Unlike point structures, a multi-span bridge extends for long distance close to the ground surface; and since an earthquake excitation is composed of a large number of waves with different amplitudes, frequencies and phases, different motions are experienced at the bridge supports. Therefore, a complete description of the ground motion requires specification of the cross correlation between the motions at different supports. The spatial variation of seismic ground motions at the multiple support systems (such as multi-span bridges or overground pipelines) may be treated deterministically or stochastically.

In the deterministic approach, two methods are commonly used, namely, the response-spectrum method and the time-history method. The single response spectrum normally used is either an amplified spectrum enveloping the response spectra for all supports or the most critical of these spectra, which results in very conservative results leading to higher construction costs. Instead, a multiple response spectrum method is used. However, it does not account for neither the cross correlation of the multiple support excitations nor the modal cross correlation of the dynamic response which can lead to significant errors in predicting the design loads. In the time-history method, a recorded time history at one support is used as the input motion and the differential motion between any two supports is estimated by considering a delay in the arrival of the seismic wave between the supports. Nelson and Weidlinger [1] developed an Interference Response Spectrum (IRS), in which any particular ordinate represents the absolute maximum out-of-phase response between two adjacent points. Somaini [2] studied the seismic behaviour of girder bridge to horizontally propagating waves (body or Rayleigh waves). The excitation is specified by the horizontal and vertical free-field motions of the ground surface in the control points and a time-dependent correlation function. Nazmy and Abdel-Ghaffar [3] utilized the step-by-step integration technique to solve the nonlinear equation of motion of long-span cable-stayed bridges subjected to multiple support excitation. Spyrakos [4] studied the seismic behavior of bridge piers assuming stiff bridge deck and including the soil-structure interaction. Harmonic

excitation is assumed and the spatial variation of ground motion is neglected. The time-history method is quite costly and more than one analysis is required to reflect the statistical trends of all possible earthquakes.

In the stochastic approach, the ground motions at different points are modelled as random processes with a given PSD function and the spatial variation is described by a cross correlation function. This approach has the advantage that the characteristics of an ensemble of possible earthquakes may be considered in one analysis and the statistical properties of maximum response can be evaluated, and consequently the probabilistic informations associated with risk levels of response can be incorporated into the design decision. Zerva et al [5,6] developed an analytical model for near source random ground motions based on the earthquake and site characteristics. The outputs of this model (power and cross spectral densities) are used to analyze the responses of pipelines and bridges subjected to either perfectly or partially correlated stationary random input motions. Abdel-Ghaffar and Rubin [7,8] analyzed the response of suspension bridges to multiple support excitations in lateral and vertical directions. The ground motions are defined through finite Fourier transforms. The supports are assumed to be rigid and follows the ground motions. A frequency domain random vibration is used to evaluate the root mean square (r.m.s) and peak responses. Lee and Penzien [9] developed a stochastic seismic analysis for structures and piping systems subjected to multiple support stationary random excitation. The cross correlation of the input excitations and that of the modal responses are considered. Zavoni and Vanmarcke [10] presented a random vibration methodology for the seismic response analysis of linear multi-support structural systems to multiple support stationary input considering the space time correlation and local spatial variation of ground motion. Soliman and Datta [11] proposed a response analysis of multi-span bridge to stationary random vertical ground motion considering the cross correlation between ground motions at different points and neglecting the soil-support interaction.

In the previous investigations [5-11] the seismic excitations were assumed as partially or fully

correlated stationary random processes of long duration. But, the recorded accelerograms of severe motion earthquakes have finite duration and strong nonstationarity in both amplitude and frequency content. Mashaly [12] developed an evolutionary spectral approach for analyzing the response of underground pipelines to multimode nonstationary random ground motion.

The soil-support interaction has considerable effect on the bridge response. Nevertheless, the literature search showed that the interaction effect was mostly ignored. The main task of soil-structure interaction problem is the evaluation of the dynamic stiffness matrix of the foundation. To find the soil impedance functions, a mixed boundary-value problem (in which displacements are prescribed due to unit harmonic load at the contact area between the foundation and the soil) is to be solved [13,14]. By fitting mathematical expressions to accurate numerical solutions, Pais and Kausel [15] proposed approximate formulas for the frequency-dependent dynamic stiffness of rigid cylindrical and rectangular embedded foundations.

In this paper, a comprehensive analysis of the seismic response of multi-support systems to multiple-support excitation is presented. The seismic excitation is represented by the three translational components of earthquake ground motions acting at the bridge supports in three orthogonal principal axes (two horizontal and one vertical). The earthquake waves are assumed to be propagating towards the longitudinal axis of bridge or incident at an angle. The ground motions are idealized as stationary or nonstationary random processes characterized by PSD or ESD and GSD functions. The spatial variation of ground motion along the bridge is incorporated using exponentially decaying correlation functions. The soil-structure interaction for rectangular rigid supports of bridge is represented by frequency-dependent impedance functions which are expressed by empirical formulas that account for the embedment depth and support dimensions. The stiffness matrix of bridge is modified to involve the effect of flexible joints. Stochastic analyses are carried out to evaluate the r.m.s and peak responses.

ANALYTICAL FORMULATION

Mathematical Model and Assumptions

The girder bridge is assumed to be elastic, continuous, (or with flexible joints) and is supported at certain intervals along its length on rectangular supports. The supports are assumed to be rigid and follow the ground motion, i.e. the ground motions at the base of supports are identical to those at the bridge deck. A discrete lumped mass model is used to describe the bridge motion (see Figure (1)), in which the bridge is discretized into $(n-1)$ 3-D beam elements (with n nodes) and the appropriate masses of the elements and supports are lumped at the nodes. The dynamic d.o.f at each node consist only of the three translations in $x, y,$ and z directions. The dynamic soil resistance to support motion is linearly proportional to the relative displacements between the soil and supports and is characterized by a spring-dashpot system (only springs are shown in Figure (1)) The bridge displacements are small in comparison to its dimensions.

Seismic Excitation

The seismic excitation is represented by three uncorrelated translational components of earthquake ground motions directed along three orthogonal principal axes (two horizontal perpendicular components u_g, v_g and one vertical w_g) with the major axes 'u' being directed towards the expected epicentre (direction of wave propagation), the moderate principal axis 'v' directed horizontally perpendicular to it, and the minor principal axis 'w' directed vertically. The relative magnitude of the three components are specified by assumed ratios. The earthquake waves are assumed to be propagating in the direction of the longitudinal axis of bridge or incident at an angle γ with a set of global axes x, y, z (Figure (1)). The components of ground motion in $x, y,$ and z directions are obtained as

$$\begin{aligned} x_g &= -u_g \cos \gamma + v_g \sin \gamma \\ y_g &= -u_g \sin \gamma - v_g \cos \gamma \\ z_g &= w_g \end{aligned} \quad (1)$$

It can be noted from Eq. 1 that the motion felt by the bridge along the global axes will be correlated.

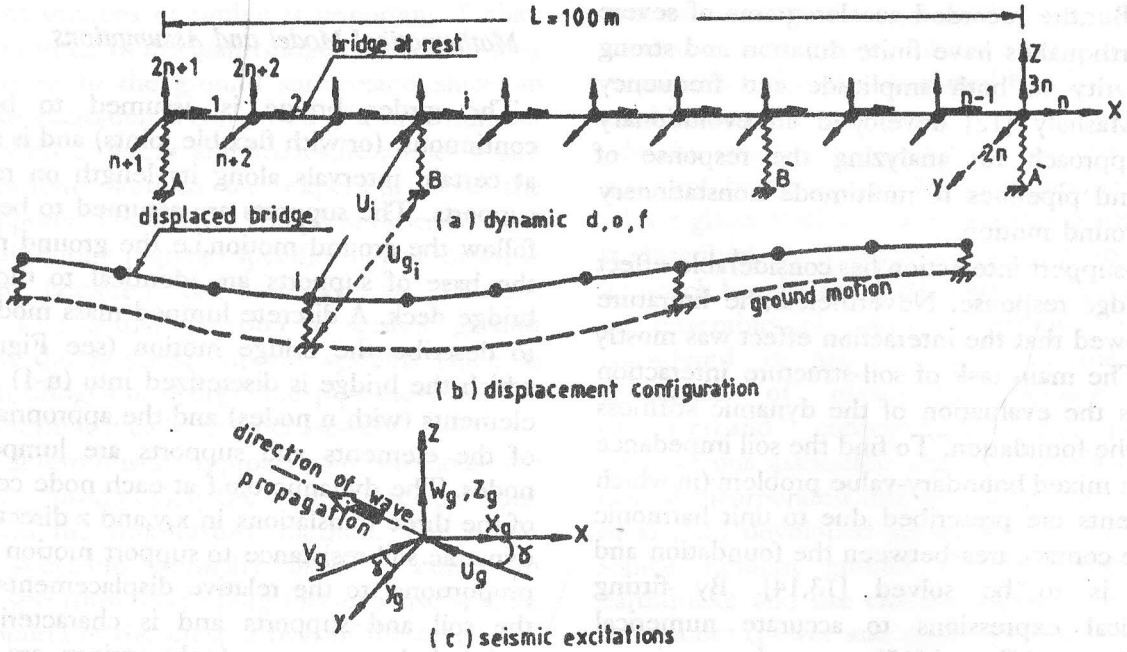


Figure 1. Mathematical model of bridge-support system and seismic excitations.

The degree of correlation depends upon the relative orientation (γ) of the bridge w.r.t the principal axes. The components of ground motion (u_g, v_g, w_g) at bridge supports are idealized as stationary or nonstationary random processes.

1- Stationary random process:

Usually, the free field ground motion is assumed to be a stationary random process with zero mean and resembles a filtered white noise of limited duration characterized by a PSD function $S_{\ddot{u}_g}(\omega)$. Several forms of the PSD functions are suggested in the literature. The modified Kanai-Tajimi PSD function proposed by Clough and Penzien [16] for the ground acceleration is utilized in the present study,

$$S_{\ddot{u}_g}(\omega) = S_{\ddot{u}_0} |H_1(i\omega)|^2 |H_2(i\omega)|^2 \quad (2)$$

where $S_{\ddot{u}_0}$ is the PSD function of white-noise bed-rock acceleration \ddot{u}_0 , $H_1(i\omega), H_2(i\omega)$ are the transfer functions of two soil filters above the bed-rock, where

$$|H_1(i\omega)|^2 = \frac{1 + (2\zeta_g \omega / \omega_g)^2}{[1 - (\omega / \omega_g)^2]^2 + (2\zeta_g \omega / \omega_g)^2} \quad (3)$$

$$|H_2(i\omega)|^2 = \frac{(\omega / \omega_f)^4}{[1 - (\omega / \omega_f)^2]^2 + (2\zeta_f \omega / \omega_f)^2}$$

ω_g, ζ_g are the resonant frequency and damping ratio of the first filter and ω_f, ζ_f are those of the second filter.

$S_{\ddot{u}_0}$ is calculated by defining the filter characteristics $\omega_g, \zeta_g, \omega_f, \zeta_f$ specifying a standard deviation for the ground acceleration $\sigma_{\ddot{u}_g}$, and using the relation

$$\sigma_{\ddot{u}_g}^2 = \int_0^\infty S_{\ddot{u}_g}(\omega) d\omega \quad (4)$$

for the variance of process $\ddot{u}_g(t)$ defined by the one-sided spectrum, $S_{\ddot{u}_g}(\omega)$

2- Nonstationary random process:

Many nonstationary models have been suggested; in most of them, a nonstationary random process $\ddot{u}_g(t)$ is represented by the product of stationary zero-mean random process $\bar{u}_g(t)$ and a deterministic uniformly modulated (or envelope) function $A(t)$ of arbitrary shape which includes the nonstationary effect in amplitude (neglecting the nonstationary nature of frequency content), i.e

$$\ddot{u}_g(t) = A(t)\bar{u}_g(t) \tag{5}$$

Four typical increasing-decreasing envelope functions are presented schematically in Figure (2), in which the parameters $t_1, t_2, a_1, a_2, b_1, b_2, c,$ and \bar{a}_0 are adjusted by the magnitude and duration of earthquake, epicentral distance, and shape of time history of earthquake ground motion.

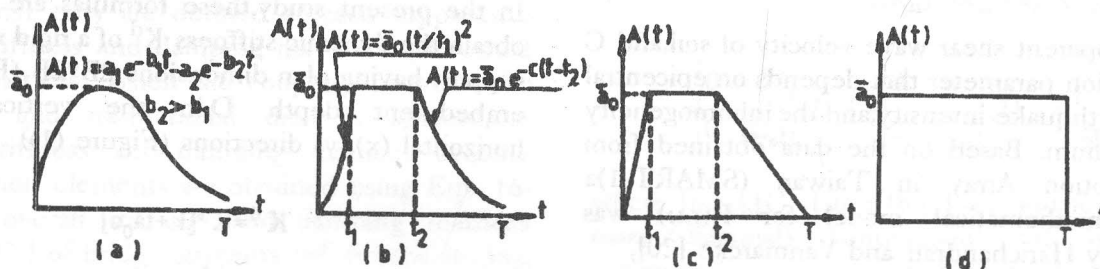


Figure 2. Typical envelope modulating functions $A(t)$.

If $A(t)$ is slowly varying with the time w.r.t $\ddot{u}_g(t)$ and is repeated exactly at each record, the autocorrelation function of ground acceleration is obtained from Eq. 5 as

$$R_{\ddot{u}_g}(t_1, t_2) = A(t_1)A(t_2)R_{\bar{u}_g}(t_1 - t_2) \tag{6}$$

using Wiener-Khinchine relationship for stationary process, the autocorrelation function $R_{\ddot{u}_g}(t_1 - t_2)$ can be related to the one sided PSD function $S_{\bar{u}_g}(\omega)$, as

$$R_{\ddot{u}_g}(t_1 - t_2) = \int_0^{\infty} S_{\bar{u}_g}(\omega) e^{i\omega(t_1 - t_2)} d\omega \tag{7}$$

and $R_{\ddot{u}_g}(t_1, t_2)$ can be then rewritten as

$$R_{\ddot{u}_g}(t_1, t_2) = A(t_1)A(t_2) \int_0^{\infty} S_{\bar{u}_g}(\omega) e^{i\omega(t_1 - t_2)} d\omega \tag{8}$$

The double-frequency Generalized Spectral Density (GSD) function of $\ddot{u}_g(t)$ is then given as [17]

$$S_{\ddot{u}_g}(\omega_1, \omega_2) = \frac{1}{4\pi^2} \int_{-\infty}^{\infty} \int_{-\infty}^{\infty} R_{\ddot{u}_g}(t_1, t_2) e^{-i(\omega_1 t_1 - \omega_2 t_2)} dt_1 dt_2 \tag{9}$$

or from Eq. 8, it follows as

$$S_{\ddot{u}_g}(\omega_1, \omega_2) = \frac{1}{4\pi^2} \int_{-\infty}^{\infty} \int_{-\infty}^{\infty} A(t_1)A(t_2) \int_0^{\infty} S_{\bar{u}_g}(\omega) e^{i\omega(t_1 - t_2)} e^{-i(\omega_1 t_1 - \omega_2 t_2)} d\omega dt_1 dt_2 \tag{10}$$

On the other hand, Mashaly [12] employed the approach developed by Priestley [18] to describe a procedure for finding an expression for the Evolutionary (time-dependent) Spectral Density (ESD) function (with the help of Eq. 5) as

$$S_{\ddot{u}_g}(\omega, t) = A^2(t)S_{\bar{u}_g}(\omega) \tag{11}$$

The spatial variation of seismic ground motions at the multiple support is accounted for using a cross correlation function $R(r, \omega)$. Thus, the cross spectrum of ground acceleration between two points can be given as

$$S_{\ddot{u}_g}(r, \omega) = S_{\ddot{u}_g}(\omega) R(r, \omega) \quad (12)$$

in which $S_{\ddot{u}_g}(\omega)$ is the local spectrum of ground acceleration (Eq. 2). The studies in the literature showed that, $R(r, \omega)$ at two stations y_1, y_2 decays with the increase of the separation distance $r = |y_1 - y_2|$ between them, and the frequency ω . Hindy and Novak [19] proposed the following form

$$R(r, \omega) = \exp\left[-C \frac{r\omega}{2\pi V_s}\right] \quad (13)$$

V_s is the apparent shear wave velocity of soil, and C is a correlation parameter that depends on epicentral distance, earthquake intensity, and the inhomogeneity of the medium. Based on the data obtained from Strong Motion Array in Taiwan (SMART-1) a tentative mathematical model for $R(r, \omega)$ was proposed by Harichandran and Vanmarcke [20],

$$R(r, \omega) = A_1 \exp\left(-\frac{\beta}{\alpha}\right) + (1 - A_1) \exp(-\beta),$$

$$\beta = 2r(1 - A_1 + \alpha A_1) / \theta(\omega) \quad (14)$$

$$\theta(\omega) = \bar{K} \sqrt{1 + (\omega/\omega_0)^{b_1}}$$

$A_1, \alpha, \bar{K}, \omega_0,$ and b_1 are parameters estimated from the data. Loh [21] used the SMART-1 array data to develop mathematical models for the spatial correlation coefficients of the ground motion described in the time-domain and frequency domain,

$$R(r, t) = \exp[-c_1 r] \cos 2\pi k_0 r$$

$$R(r, \omega) = \exp[-(a_1 + a_2 \omega) r] \quad (15)$$

c_1, k_0, a_1, a_2 are parameters which control the spatial correlation shape. The correlation functions given by Eqs. 13, and 14 are employed in the present study

Soil-Support Interaction

The soil-structure interaction has the effect of modifying the structural response during earthquakes. Usually, equivalent springs and dampers are used to represent the soil-structure interaction. The spring-damper constants are obtained from soil

impedance functions which are analytically determined by calculating the displacements at the contact area between a rigid footing and the soil (idealized as an elastic half space) due to unit harmonic load. The evaluation of impedance functions for various shapes of foundations, embedment depths, and soil conditions is a complex problem. Pais and Kausel [15] proposed approximate formulas for the frequency-dependent dynamic stiffness of rigid embedded foundations. These formulas are obtained by fitting mathematical expressions to accurate numerical solutions [13,14]. In the present study, these formulas are utilized to obtain the dynamic stiffness K^d of a rigid rectangular support having plan dimensions $2B \times 2B_1$ ($B \leq B_1$) and embedment depth D , in the vertical (z), and horizontal (x), (y) directions (Figure (1))

$$K^d = K^s [k + ia_0 c] \quad (16)$$

in which a_0 is a dimensionless frequency ($a_0 = \omega B/V_s$), ω = frequency of vibration, V_s = shear wave velocity in soil, k, c are stiffness and damping coefficients, respectively, and K^s designates the approximate static stiffness, where:

a- For vertical direction z :

$$K_z^s = \frac{GB}{1-\nu} [3.1(B_1/B)^{0.75} + 1.6] * [1.0 + (0.25 + \frac{0.25}{B_1/B})(D/B)^{0.8}]$$

$$k_z = 1.0 - \frac{da_0^2}{b + a_0^2}, \quad d = 0.4 + \frac{0.2}{B_1/B}, \quad b = \frac{10}{1 + 3(B_1/B - 1)} \quad (17)$$

$$c_z = 4[\bar{\alpha} B_1/B + D/B(1 + B_1/B)] * GB/K_z^s$$

b- For horizontal directions y , and x :

$$K_y^s = \frac{GB}{2-\nu} [6.8(B_1/B)^{0.65} + 2.4] * [1.0 + (0.33 + \frac{1.34}{1 + B_1/B})(D/B)^{0.8}]$$

$$k_y = 1.0 \quad (18)$$

$$c_y = 4[B_1/B + D/B(\bar{\alpha} + B_1/B)] * GB/K_y^s$$

and

$$K_x^s = [K_y^s + \frac{GB}{2-\nu} (0.8(B_1/B - 1))] * [1.0 + (0.33 + \frac{1.34}{1 + B_1/B})(D/B)^{0.8}]$$

$$k_x = 1.0 \quad (19)$$

$$c_x = 4[B_1/B + D/B(1 + \bar{\alpha} B_1/B)] * GB/K_x^s$$

c- For coupling between rocking and translation in directions x , and y :

$$K_{x\theta}^d = \frac{1}{3}(D/B)K_x^d, K_{y\theta}^d = \frac{1}{3}(D/B)K_y^d \quad (20)$$

where $\bar{\alpha} = \sqrt{2(1-\nu)/(1+2\nu)}$, ν = Poisson's ratio, G = shear modulus = $\rho_s V_s^2$, ρ_s = soil mass density.

The real and imaginary parts of Eq. 16 represent the stiffness and damping coefficients, respectively for the bridge support. If three dynamic d.o.f (translations) only are defined at each support, the support stiffness and damping may be represented by 3*3 matrices. When the coupling between the rotational and translational d.o.f is ignored, the support stiffness and damping matrices become diagonal, their elements are obtained using Eqs. 16-19. The overall stiffness and damping matrices $[K_s]$, and $[C_s]$ of bridge supports (of dimension $3n_2$, n_2 being the number of supports) are obtained by simply assembling those of the individual supports.

Since the dominant energy of earthquake excitation is confined within a low frequency range, the bridge has most of its response in this range. Thus, in Eq. 17, the frequency dependence of support stiffness can be neglected i.e $k_z = 1.0$

Bridge Stiffness Matrix $[K_b]$

The standard form of the stiffness matrix for individual 3-D beam element is modified to introduce the effect of flexible joints (if any) as explained in Refs. [22,23]. The stiffness matrices of different bridge elements are transformed into the global coordinates and then assembled to achieve the overall stiffness matrix of the entire bridge corresponding to kinematic d.o.f ($6n$), n being the number of nodes. This stiffness matrix is rearranged and partitioned into submatrices $[K_{\theta\theta}]$, $[K_{\theta\Delta}]$, $[K_{\Delta\theta}]$ and $[K_{\Delta\Delta}]$ in which (θ) and (Δ) are the rotations and translations at the nodes of bridge in global coordinates. The stiffness matrix of bridge corresponding to dynamic d.o.f ($3n$) is obtained by matrix condensation as

$$[K_b] = [K_{\Delta\Delta}] - [K_{\Delta\theta}][K_{\theta\theta}]^{-1}[K_{\theta\Delta}]^T \quad (21)$$

Equation of Motion

The equations of motion of the bridge-support system subjected to multiple support excitations can be written in a matrix form of order $3n$ in terms of absolute displacements as

$$\begin{bmatrix} [m_{11}] & 0 \\ 0 & [m_{22} + m_s] \end{bmatrix} \begin{Bmatrix} (\ddot{U}_1) \\ (\ddot{U}_2) \end{Bmatrix} + \begin{bmatrix} [C_{11}] & [C_{12}] \\ [C_{21}] & [C_{22} + C_s] \end{bmatrix} \begin{Bmatrix} (\dot{U}_1) \\ (\dot{U}_2) \end{Bmatrix} + \begin{bmatrix} [K_{11}] & [K_{12}] \\ [K_{21}] & [K_{22} + K_s] \end{bmatrix} \begin{Bmatrix} (U_1) \\ (U_2) \end{Bmatrix} = \begin{bmatrix} 0 & 0 \\ 0 & [C_g] \end{bmatrix} \{\dot{U}_g\} = \begin{bmatrix} 0 & 0 \\ 0 & [K_g] \end{bmatrix} \{U_g\} = \begin{Bmatrix} 0 \\ \{p(t)\} \end{Bmatrix} \quad (22)$$

where $[m_{11}]$, $[C_{11}]$, and $[K_{11}]$ are square matrices of mass (diagonal), damping, and stiffness of bridge corresponding to nonsupport d.o.f ($3n_1$); $[m_{22}]$, $[C_{22}]$, and $[K_{22}]$ are those corresponding to support d.o.f ($3n_2$); $[C_{12}]$, and $[K_{12}]$ are matrices of the bridge damping and stiffness denoting the coupling between nonsupport and support d.o.f; $[C_{21}]$, and $[K_{21}]$ are their transpose; $[C_s]$, $[K_s]$ are diagonal matrices of damping and stiffness of bridge supports of size $3n_2$; (\ddot{U}_1) , (\dot{U}_1) , and (U_1) are the vectors of absolute values of bridge accelerations, velocities and displacements at nonsupport d.o.f; (\ddot{U}_2) , (\dot{U}_2) , and (U_2) are those at support d.o.f; and (\dot{U}_g) , (U_g) are vectors of ground velocities and ground displacements in the direction of d.o.f at the supports ($3n_2$).

Equation 22 can be rewritten in a simplified form as:

$$\begin{aligned} [\bar{M}](\ddot{U}) + [\bar{C}](\dot{U}) + [\bar{K}](U) &= [\bar{C}_s](\dot{U}_g) + [\bar{K}_s](U_g) = \{P(t)\} \\ \text{where} & \\ \{P(t)\} &= [\bar{C}_s](\dot{U}_g) + [\bar{K}_s](U_g) \end{aligned} \quad (23)$$

in which $[\bar{M}]$, $[\bar{C}]$, and $[\bar{K}]$ are the total mass, damping and stiffness matrices of bridge-support system; and $[\bar{K}_s]$, $[\bar{C}_s]$ are diagonal matrices having nonzero elements corresponding to support points only.

It should be noted that, the vertical component w_g of ground motion always coincides with the vertical axis z and it has no correlation with the other two

horizontal components in x and y directions. Consequently, the vertical vibration of bridge could have been obtained independent of the vibrations on the horizontal plane. This would have resulted in 2n coupled equations of motion for responses in horizontal plane and a separate set of n coupled equations for vertical response. This will lead to a considerable reduction of the computation effort.

Since the damping matrix of bridge [C_b] can be defined only in terms of modal damping, the solution of Eq. 23 can be best obtained using the normal modes of structure. However, using the normal mode theory, the left hand side of Eq. 23 can not be completely decoupled, since the normal modes are not orthogonal w.r.t [C_s]. However, a diagonal matrix of damping coefficients (e) denoting approximate modal damping of bridge supports may be obtained using energy consideration, in which e_i is defined as

$$e_i = (\phi_i)^T \begin{bmatrix} 0 & 0 \\ 0 & [C_s] \end{bmatrix} (\phi_i) / 2\omega_i \quad (24)$$

where ω_i, (φ_i) are the ith natural frequency and normalized mode shape, which are obtained by solving the equation of undamped free vibration.

Now, using the normal mode theory with the transformation (U)=[φ](Z), Eq. 23 is reduced to

$$\ddot{Z}_i + 2\eta_i \omega_i \dot{Z}_i + \omega_i^2 Z_i = (\phi_i)^T (P(t)) = f_i(t), i=1,2,\dots,q \quad (25)$$

where Z_i and f_i are the ith modal coordinate and modal force, q is the number of modes considered in the analysis, η_i=e_i+ζ_i

RESPONSE ANALYSIS

Stationary Random Excitation

If the seismic excitation is assumed as stationary random processes with zero-means, and the bridge-support system is linear, the structural responses will be also stationary random processes with zero means. The PSD functions of the responses {R(t)} can be related to the PSD functions of exciting forces {p(t)} using the standard expression

$$[S_{RR}(\omega)] = [H(i\omega)]^* [S_{pp}(\omega)] [H(i\omega)]^T \quad (26)$$

in which [S_{RR}(ω)] is the matrix of PSD functions of the responses, [S_{pp}(ω)] is that of exciting forces (will be calculated later), [H(iω)] is the matrix of complex frequency response functions which varies and depends upon the response quantities to be calculated, and *, T denote the complex conjugate and transpose, respectively. [H(iω)]_Δ for translations is obtained as

$$[H(i\omega)]_{\Delta} = [\phi][\Lambda][\phi]^T \quad (27)$$

where [Λ] is a diagonal matrix of transfer functions, its elements are obtained by finding the response to exciting force e^{iωt} applied in the direction of each dynamic d.o.f in succession. The response to e^{iωt} applied in the direction of ith dynamic d.o.f is obtained by solving Eq. 25 in the frequency domain with {f(t)} changed to {f(t)}={0 0 ... e^{iωt} 0 0}^T, e^{iωt} is the ith element of {f(t)}. Λ_i is then obtained as

$$\Lambda_i = [(\omega_i^2 - \omega^2) - i(2\omega_i \omega \eta_i)] / [(\omega_i^2 - \omega^2)^2 + (2\omega_i \omega \eta_i)^2] \quad (28)$$

[H(iω)]_f for the internal forces can be obtained directly from [H(iω)]_Δ by simply finding [H(iω)]_θ for rotations using the relation

$$[H(i\omega)]_{\theta} = -[K_{\theta\theta}]^{-1} [K_{\Delta\theta}] [H(i\omega)]_{\Delta} \quad (29)$$

then the standard method of analysis is utilized to obtain the columns of [H(iω)]_f, where the vectors {Δ}_i(θ)_i are replaced by {H(iω)}_Δⁱ, {H(iω)}_θⁱ.

Calculation of [S_{pp}(ω)]:

As stated earlier, the seismic excitation is represented by three uncorrelated translation components of earthquake ground motions u_g, v_g, and w_g acting at the support points in the principal directions u, v, w. (U_g) in Eq. 23 contains the ground displacements x_g, y_g, z_g measured in the global directions x, y, z, which are related to u_g, v_g, w_g using Eq. 1. Since u_g, v_g, w_g are uncorrelated (i.e. S_{ug vg} = S_{ug wg} = S_{vg wg} = 0.0), the PSD and cross SD functions in global directions x, y, z are obtained as

$$\begin{aligned}
 S_{x_i x_j}(\omega) &= \cos^2 \gamma S_{u_i}(\omega) + \sin^2 \gamma S_{v_i}(\omega) \\
 S_{y_i y_j}(\omega) &= \sin^2 \gamma S_{u_i}(\omega) + \cos^2 \gamma S_{v_i}(\omega) \\
 S_{z_i z_j}(\omega) &= S_{w_i}(\omega) \\
 S_{x_i y_j}(\omega) &= S_{y_i x_j}(\omega) = \sin \gamma \cos \gamma (S_{u_i}(\omega) - S_{v_i}(\omega))
 \end{aligned}
 \tag{30}$$

$[S_{pp}(\omega)]$ is directly derived using the principles of spectral analysis, as

$$\begin{aligned}
 [S_{pp}(\omega)] &= [C_s][S_{\dot{u}_i \dot{u}_i}(\omega)][C_s]^T + [C_s][S_{\dot{u}_i \dot{v}_i}(\omega)][K_s]^T + \\
 & [K_s][S_{\dot{v}_i \dot{u}_i}(\omega)][C_s]^T + [K_s][S_{\dot{v}_i \dot{v}_i}(\omega)][K_s]^T
 \end{aligned}
 \tag{31}$$

The matrices of PSD functions in Eq. 31 will involve the cross spectral density functions

$$\begin{aligned}
 S_{\dot{x}_i \dot{x}_j}, S_{\dot{x}_i \dot{y}_j}, S_{\dot{y}_i \dot{x}_j}, S_{\dot{y}_i \dot{y}_j}, S_{\dot{x}_i \dot{z}_j}, S_{\dot{x}_i \dot{w}_j}, S_{\dot{y}_i \dot{z}_j}, S_{\dot{y}_i \dot{w}_j}, S_{\dot{z}_i \dot{z}_j}, \\
 S_{\dot{z}_i \dot{w}_j}, \text{etc.....} i, j = 1, 2, \dots, n
 \end{aligned}$$

Assuming local ground displacements spectra $S_{x_g x_g}, S_{x_g y_g}, S_{x_g z_g}$ and $S_{z_g z_g}$ to be the same for all stations, using Eq. 13 or Eq. 14 to express the cross correlation $R_{ij}(r, \omega)$ of displacements between two stations i, j , and utilizing the rules of stochastic analysis, the above cross spectral density functions can be expressed in terms of $S_{u_i}, S_{v_i}, S_{w_i}$, angle of incidence γ and $R_{ij}(r, \omega), i, j = 1, \dots, n$ with the help of Eq. 30, e.g

$$\begin{aligned}
 S_{\dot{x}_i \dot{x}_j} &= (-i\omega)R_{ij}(r, \omega)S_{x_i x_j} \\
 S_{\dot{x}_i \dot{y}_j} &= (i\omega)R_{ij}(r, \omega)S_{x_i x_j}
 \end{aligned}
 \tag{32}$$

and so on

The root mean square value of the response quantity $R_i(t)$ (equals the standard deviation σ_{R_i} for zero mean process) is calculated from the one-sided PSD function $S_{R_i R_i}(\omega)$ as

$$\text{r.m.s}(R_i(t)) = \sigma_{R_i} = \sqrt{\int_0^{\infty} S_{R_i R_i}(\omega) d\omega}
 \tag{33}$$

Nonstationary Random Excitation:

Two alternative spectral methods are presented

herein for obtaining the mean-square response of multi-support system to nonstationary random excitation namely, the double frequency generalized spectra method, and the evolutionary spectra method.

(i) Double Frequency Generalized Spectra Method

Again, since the multi-support system is linear and the seismic excitations are nonstationary random processes, with zero means, the system responses will be nonstationary random processes with zero means. Using the modal coordinates $\{Z\}$ given by Eq. 25, the transformation $\{U\} = [\phi]\{Z\}$, and the principles of stochastic analysis, the matrix of covariance functions of translations can be obtained as,

$$[R_{uu}(t_1, t_2)] = \int \int_{-\infty}^{\infty} [H(i\omega_1)]_{\Delta}^* [S_{pp}(\omega_1, \omega_2)] [H(i\omega_2)]_{\Delta}^T e^{i(\omega_1 t_1 - \omega_2 t_2)} d\omega_1 d\omega_2
 \tag{34}$$

in which $[H(i\omega)]_{\Delta}$ is the matrix of complex frequency response functions of translations that is defined by Eqs. 27, 28, and $[S_{pp}(\omega_1, \omega_2)]$ is the matrix of double-frequency GSD functions of exciting force $\{P(t)\}$ (Eq. 9). Note that, the matrix of covariance functions of forces response is obtained using an equation similar to Eq. 34 by replacing $[H(i\omega)]_{\Delta}$ by $[H(i\omega)]_f$ of forces.

Now, if the ground motions $\{\ddot{U}_g\}, \{\dot{U}_g\}, \{U_g\}$ are considered nonstationary random processes described by Eq. 5, the vector of ground displacements (for example) can be written as

$$\{U_g(t)\} = [A(t)]\{\bar{U}_g(t)\}$$

where $[A(t)]$ is a diagonal matrix of envelope functions and $\{U_g(t)\}$ is a vector of stationary random processes. Accordingly, Eq. 23 is rewritten as

$$\begin{aligned}
 \{P(t)\} &= [\bar{C}_s][A(t)]\{\dot{U}_g\} + [\bar{K}_s][A(t)]\{U_g\} = [A(t)]\{\bar{P}(t)\} \\
 \text{with} & \\
 \{\bar{P}(t)\} &= [\bar{C}_s]\{\dot{U}_g\} + [\bar{K}_s]\{U_g\}
 \end{aligned}
 \tag{35}$$

Using Eqs. 35, 6, the matrix of covariance functions of nonstationary random excitations $\{P(t)\}$ can be related to that of stationary random excitations $\{P(t)\}$

as

$$[R_{pp}(t_1, t_2)] = [A(t_1)][R_{pp}(t_1 - t_2)][A(t_2)]^T \quad (36)$$

The matrix of double-frequency GSD function, $[S_{pp}(\omega_1, \omega_2)]$ is obtained using Eqs. 36,9 as

$$[S_{pp}(\omega_1, \omega_2)] = \frac{1}{4\pi^2} \int_{-\infty}^{\infty} \int_{-\infty}^{\infty} [A(t_1)][R_{pp}(t_1 - t_2)][A(t_2)]^T e^{-i(\omega_1 t_1 - \omega_2 t_2)} dt_1 dt_2 \quad (37)$$

Moreover, $[S_{pp}(\omega_1, \omega_2)]$ can be obtained as a function of $[S_{pp}(\omega)]$, the matrix of PSD functions of stationary random exciting force $[P(t)]$ using Eq.7,i.e

$$[S_{pp}(\omega_1, \omega_2)] = \frac{1}{4\pi^2} \int_{-\infty}^{\infty} \int_{-\infty}^{\infty} [A(t_1)] \left\{ \int_0^{\infty} [S_{pp}(\omega)] e^{i\omega(t_1 - t_2)} d\omega \right\} [A(t_2)] e^{-i(\omega_1 t_1 - \omega_2 t_2)} dt_1 dt_2 \quad (38)$$

Since $A(t)=0$ if $t_1 < t < 0$, and the integrals in the above equation are convergent (i.e any process has finite energy), the order of the integrals may be reversed and the limits are changed, then Eq. 38 becomes

$$[S_{pp}(\omega_1, \omega_2)] = \int_0^{\infty} \left\{ \frac{1}{2\pi} \int_0^t [A(t_1)] e^{i(\omega - \omega_1)t_1} dt_1 [S_{pp}(\omega)] \right. \\ \left. \frac{1}{2\pi} \int_0^t [A(t_2)] e^{-i(\omega - \omega_2)t_2} dt_2 \right\} d\omega \quad (39)$$

or

$$[S_{pp}(\omega_1, \omega_2)] = \int_0^{\infty} [J_1(\omega - \omega_1)]^* [S_{pp}(\omega)] [J_2(\omega - \omega_2)] d\omega \quad (40)$$

with

$$[J_1(\omega - \omega_1)]^* = \frac{1}{2\pi} \int_0^t [A(t_1)] e^{i(\omega - \omega_1)t_1} dt_1, \quad (41)$$

$$[J_2(\omega - \omega_2)] = \frac{1}{2\pi} \int_0^t [A(t_2)] e^{-i(\omega - \omega_2)t_2} dt_2$$

from Eqs. 40, and 34, $[R_{uu}(t_1, t_2)]$ can be given by

$$[R_{uu}(t_1, t_2)] = \int_0^{\infty} \int_{-\infty}^{\infty} [H(i\omega_1)]^* [J_1(\omega - \omega_1)]^* [S_{pp}(\omega)] [J_2(\omega - \omega_2)] [H(i\omega_2)]^T e^{i(\omega_1 t_1 - \omega_2 t_2)} d\omega_1 d\omega_2 d\omega \quad (42)$$

Eventually, the time-dependent mean-square response $E[u^2(t)]$ is obtained from Eq.42 by setting $t_1 = t_2 = t$, i.e

$$[E[u^2(t)]] = [R_{uu}(t, t)] = \int_0^{\infty} [I(t, \omega)]^* [S_{pp}(\omega)] [I(t, \omega)]^T d\omega \quad (43)$$

in which $[I(t, \omega)]$ is the matrix of time-dependent complex frequency response functions and is defined as

$$[I(t, \omega)]^* = \int_{-\infty}^{\infty} [H(i\omega_1)]^* [J(\omega - \omega_1)]^* e^{i\omega_1 t} d\omega_1, \quad (44)$$

$$[I(t, \omega)]^T = \int_{-\infty}^{\infty} [J(\omega - \omega_2)] [H(i\omega_2)]^T e^{-i\omega_2 t} d\omega_2$$

(ii) Evolutionary Spectra Method

Equation 25 can be solved in time domain using Duhamel's integral. For zero initial condition, the modal coordinates are given as

$$Z_i(t) = \int_0^t h_i(t-\tau) f_i(\tau) d\tau \quad i=1,2,\dots,q \quad (45)$$

in which $h_i(t-\tau)$ is the i th unit-impulse response function defined as

$$h_i(t-\tau) = \frac{1}{\omega_{d_i}} \exp[-\eta_i \omega_i (t-\tau)] \sin \omega_{d_i} (t-\tau) \quad \eta_i \leq 1,$$

$$h_i(t-\tau) = \frac{1}{2\omega_{e_i}} \exp[-\eta_i \omega_i (t-\tau)] [e^{\omega_{e_i} (t-\tau)} - e^{-\omega_{e_i} (t-\tau)}] \quad \eta_i \geq 1 \quad (46)$$

$$\text{with } \omega_{d_i} = \omega_i \sqrt{1 - \eta_i^2}, \quad \omega_{e_i} = \omega_i \sqrt{\eta_i^2 - 1}$$

If the ground motions are considered zero-mean uniformly modulated nonstationary random processes, expressed by Eq. 5, then using the modal coordinates $\{Z\}$, the transformation $\{U\} = [\phi]\{Z\}$ and the principles of evolutionary spectral analysis

developed in Ref. [12], the covariance matrix of the displacement response {U} can be calculated as

$$[R_{uu}(t_1, t_2)] = \int_0^{\infty} [\phi][B(t_1, \omega)]^* [\phi]^T [S_{pp}(\omega)] [\phi][B(t_2, \omega)][\phi]^T d\omega \quad (47)$$

where [B(t, ω)] is a diagonal matrix of modulated impulse-response functions given as

$$[B(t, \omega)] = \int_0^t [A(\tau)][h(t-\tau)]e^{-i\omega\tau} d\tau \quad (48)$$

its elements are evaluated numerically (Ref. [12]).

The time-dependent mean-square displacements [E[u²(t)]] (same as variances [σ_u²(t)]) are obtained by setting t₁=t₂=t in Eq. 47,

$$[E[U^2(t)]] = [\sigma_u^2(t)] = \int_0^{\infty} [Q^*(t, \omega)][S_{pp}(\omega)][Q(t, \omega)]^T d\omega \quad (49a)$$

or

$$[E[U^2(t)]] = [\sigma_u^2(t)] = \int_0^{\infty} [S_{uu}(t, \omega)] d\omega \quad (49b)$$

in which, [S_{uu}(t, ω)] is the matrix of ESD functions of the response vector {U(t)}, where

$$[S_{uu}(t, \omega)] = [Q(t, \omega)]^* [S_{pp}(\omega)] [Q(t, \omega)]^T \quad (50a)$$

and

$$[Q(t, \omega)]^* = [\phi][B(t, \omega)]^* [\phi]^T, [Q(t, \omega)]^T = [\phi][B(t, \omega)][\phi]^T \quad (50b)$$

The time-dependent mean square forces [E[f²(t)]] = [σ_f²(t)] are obtained using equations similar to Eqs.50 in which [φ] (not [φ]^T) is replaced by [ψ] the matrix of mode shapes of forces which is obtained using the standard method of analysis with the help of [φ] and the relation (θ) = -[K_{θθ}]⁻¹[K_{Δθ}](Δ)

Statistical Properties of Maximum Response

In many design problems, it is necessary to evaluate the peak structural response. The peak value of a random process is a random variable, its mean value and standard deviation are important to defining the

risk level in the seismic risk analysis and design decision of structures. Consider the random force process {f(t)}; the peak value of f(t) during the time interval T is defined by

$$f_{max}(T) = \max |f(t)| \quad 0 < t < T \quad (51)$$

The probability distribution, F_{f_{max}}(α) of f_{max}(T) is given as

$$F_{f_{max}}(\alpha) = P[f_{max} \leq \alpha] \quad (52)$$

which is closely related to the probability distribution L_{tf}(T) of the first passage time T_f (that is defined as the time at which f_{max}(T) crosses a level α (Figure (3)) for the first time).i.e

$$F_{f_{max}}(\alpha) = L_{T_f}(T) \quad (53)$$

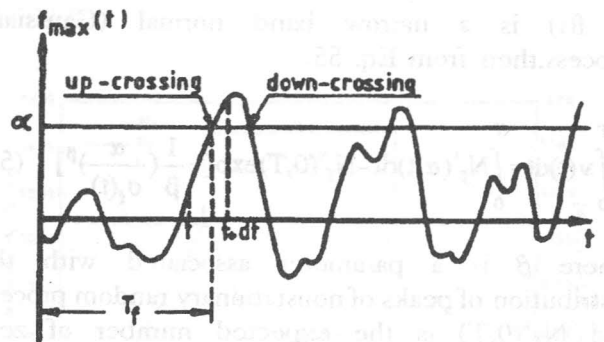


Figure 3. The first passage time T_f

Consider that the number of upcrossing f_{max} of level α in the time interval (0, T) is a nonhomogeneous Poisson's random process. The probability distribution of n upcrossings is given as [24]

$$P(n, T) = \frac{1}{n!} \left[\int_0^T \nu(t) dt \right]^n \exp \left[- \int_0^T \nu(t) dt \right] \quad (54)$$

where ν(t) is the rate of level α crossings, or the probability density in time of crossing the level f_{max}=α with a positive slope at time t,

$$v(t) = N_{f_{max}}^+(\alpha, t) = \int_0^{\dot{f}_{max}} p(\alpha, \dot{f}_{max}, t) d\dot{f}_{max} \quad (55)$$

where $\int_0^{\dot{f}_{max}} dt = \alpha - f_{max}$

The probability distribution of no crossing in interval (0,T) is

$$P(0,T) = P_0 \exp\left(-\int_0^T v(t) dt\right) \quad (56)$$

which is called also the probability distribution $L_{Tf}(T)$ of the first passage time, where $P_0 = P(T_f > 0) =$ probability of survival at $t=0$ (note that: $P_0 \equiv 1.0$ for high value of α).

From Eqs. 53,56,

$$F_{f_{max}}(\alpha) = \exp\left(-\int_0^T v(t) dt\right) \quad , P_0 = 1 \quad (57)$$

If $f(t)$ is a narrow band normal (Gaussian) process, then from Eq. 55,

$$\int_0^T v(t) dt = \int_0^T N_{f_{max}}^+(\alpha, t) dt = N_{f_{max}}^+(0, T) \exp\left[-\frac{1}{\beta} \left(\frac{\alpha}{\sigma_f(t)}\right)^\beta\right] \quad (58)$$

where β is a parameter associated with the distribution of peaks of nonstationary random process and $N_{f_{max}}^+(0, T)$ is the expected number of zero crossing in interval (0,T), where

$$N_{f_{max}}^+(0, T) = \int_0^T N_{f_{max}}^+(0, t) dt \quad , \quad (59)$$

$$N_{f_{max}}^+(0, t) = \frac{1}{2\pi} \frac{\sigma_f(t)}{\sigma_f(t)} = \frac{1}{2\pi} \sqrt{\frac{\lambda_2(t)}{\lambda_0(t)}}$$

$\lambda_0(t), \lambda_2(t)$ are the first and third moments of the time-dependent ESD function $S_f(\omega, t)$ and can be evaluated from the relation

$$\lambda_m(t) = \int_0^\infty \omega^m S_f(\omega, t) d\omega \quad (60)$$

substitution from Eq.58 into Eq.57 yields

$$F_{f_{max}}(\alpha) = \exp\left\{-N_{f_{max}}^+(0, T) \exp\left[-\frac{1}{\beta} \left(\frac{\alpha}{\sigma_f(t)}\right)^\beta\right]\right\}$$

$$= \exp\left\{-\exp\left[-D_1^{\beta-1} \left(\frac{\alpha}{\sigma_f(t)} - D_1\right)\right]\right\} \quad (61)$$

where

$$D_1 = [\beta \ln(N_{f_{max}}^+(0, T))]^{1/\beta} \quad (62)$$

The mean peak value $E[f_{max}(T)]$ of $f_{max}(t)$ can be obtained as [25]

$$E[f_{max}(t)] = \mu_{f_{max}} = K_{f_{max}}(t) \sigma_f(t) \quad (63)$$

where $K_{f_{max}}(t)$ is the time-dependent peak factor given as

$$K_{f_{max}}(t) = D_1 + \frac{0.5772}{D_1} \quad (64)$$

and the standard deviation $\sigma_{f_{max}}(t)$ of $f_{max}(t)$ is also given as

$$\sigma_{f_{max}}(t) = \frac{\pi}{\sqrt{6}} \frac{\sigma_f(t)}{D_1^\beta} \quad (65)$$

Note that: for stationary random force process $f(t)$, same procedure described above can be used, in which the integral $(\int v(t) dt)$ is replaced by $(v \cdot T)$, and $\beta=2$ in Eqs. 58,61, and 62; accordingly D_1 in Eqs. 62, 64, and 65 becomes

$$D_1 = [2 \ln(N_{f_{max}}^+(0, T))]^{1/2} \quad , \quad N_{f_{max}}^+(0) = \frac{1}{2\pi} \frac{\sigma_f}{\sigma_f} = \frac{1}{2\pi} \sqrt{\frac{\lambda_2}{\lambda_0}} \quad (66)$$

$$\lambda_m = \int_0^\infty \omega^m S_f(\omega) d\omega$$

NUMERICAL RESULTS

Employing the analysis methods proposed in the previous sections, a computer programme is developed by the author. Using this programme an extensive numerical study is conducted to

investigate the seismic behavior of multi-span girder bridges and the influence of some important factors on their responses. The three-span bridge shown in Figure (1) is analyzed to conduct the numerical study. The following input data are used:

Bridge and Support Data: Mass density $\rho_b=0.25(t/m^3)/(m/sec^2)$; modulus of elasticity $E=3*10^6 t/m^2$; bridge length $L=100m$ or varied; cross-section properties are $A=4.8m^2, I_x=3.6 m^4, I_y=1.024 m^4$ or varied; modal damping ratio of bridge material $\zeta=0.05$ and is common for all modes; the ratios between joint rigidity to bridge rigidity, $r_x=(EI_x)_j/(EI_x)_b =1.0, r_y=(EI_y)_j/(EI_y)_b =1.0, r_a=(EA)_j/(EA)_b =1.0$ or varied; shape ratio of rectangular support $B_1/B=2$ or varied; and embedment depth $D=2m$ or varied.

Soil Data: Mass density $\rho_s =0.1628(t/m^3)/(m/sec^2)$; shear wave velocity $V_s=69 m/sec$ or variable; shear modulus $G_s=V_s^2 * \rho_s$, and Poisson's ratio $\nu_s =0.33$.

Seismic Input: The seismic excitation is represented by the three uncorrelated components of earthquake ground motions acting in the principal directions u,v,w . The PSD function $S_{\ddot{u}g}(\omega)$ of stationary ground acceleration in the major direction u is obtained using Eqs. 2-4 for a standard deviation of ground acceleration $\sigma_{\ddot{u}g}=0.61 m/sec^2$ and the characteristics of filters representing soft soil condition ($V_s=69 m/sec, \omega_g=2\pi, \omega_f=0.2\pi, \zeta_g=\zeta_f=0.4$). The nonstationary ground acceleration in the major direction u is defined (with the help of Eq.5) in terms of the stationary ground acceleration and envelope function $A(t)$ which is assumed same for all the ensemble. The envelope function shown in Figure (2c) is employed herein. The double frequency GSD function $S_{\ddot{u}g}(\omega_1, \omega_2)$ and the ESD function $S_{\ddot{u}g}(\omega, t)$ are obtained using Eqs. 10 and 11, respectively. The PSD functions of ground accelerations in the moderate and minor principal directions are defined by $S_{\ddot{v}g}(\omega)=0.75 S_{\ddot{u}g}(\omega), S_{\ddot{w}g}(\omega)=0.5 S_{\ddot{u}g}(\omega)$, respectively. Equation 13 is used for defining the cross correlation function $R(t, \omega)$ between any two stations, in which the parameter C is adjusted ($C/V_s =0.0091$) to reflect the same degree of correlation when Eq. 14 is used. The earthquake waves are assumed to be propagating in the direction of the longitudinal axis of the bridge or incident at an angle γ with it.

The bridge length ($L=100 m$) is divided into different number of equal elements (7,10,13,17) with element lengths $l=14.28, 10, 7.69$ and $5.88 m$. Table

(1) shows that the internal forces at interior supports attain stationary values for element length $l \leq 10 m$. Therefore, the analyzed bridge (of length $L=100m$) is divided into 10 elements ($n=11$) of length $l=10m$

Table 1. Effect of element length l

element length (m)	M_x (t.m)	M_y (t.m)	N (ton)
14.28	1056	462	1492
10.00	1064	467	1466
7.69	1068	470	1469
5.88	1069	471	1470

The distribution of root mean square (r.m.s) values of internal forces along the bridge length is shown in Figure (4), from which it can be noted that maximum internal forces are produced at the interior supports.

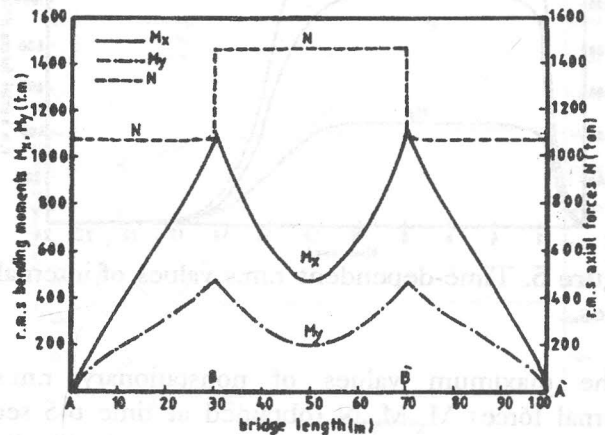


Figure 4. Distribution of internal forces along bridge length.

The r.m.s values of bridge responses to nonstationary excitations are obtained using the evolutionary spectra method and the double frequency generalized spectra method. The internal forces obtained are the same for the two. However, the second method consumed much more computational time. Therefore, the first method is employed in the rest of this study.

Effect of Nonstationarity and Duration of Earthquake Ground Motion

The time-dependent r.m.s values of internal forces at the interior support are obtained using two envelope functions (see Figure (2c)) with $t_1=2, t_2=5, T=10$ sec for envelope 1 and, $t_1=2, t_2=10, T=15$ sec for envelope 2). Figure (5) shows the time-dependent r.m.s values of bending moments (M_x, M_y) and axial forces (N), using envelope 2, from which it is seen that these forces reach their maximum values at a time $t=4$ sec and remain fairly constant up to $t=10$ sec (the time at which the envelope function begins to decline), then they decrease in a similar way as the envelope function and diminish at time $t=20$ sec. The peak factors increase with the time up to $t=11$ sec (envelope 1) and $t=16$ sec (envelope 2), then remain constant.

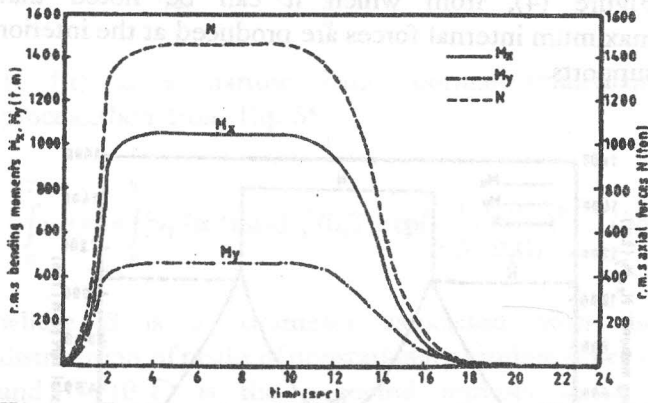


Figure 5. Time-dependent r.m.s values of internal forces.

The maximum values of nonstationary r.m.s internal forces M_x, M_y, N (obtained at time $t=5$ sec for envelope 1 and $t=10$ sec for envelope 2 with the corresponding peak factors and mean peak values (Eq. 64) are listed in Table (2). The r.m.s internal forces and their peak factors obtained due to stationary excitation of duration $T=26$ sec are also given for the sake of comparison. Referring to the mean peak values of internal forces, it is noted that the nonstationary internal forces (envelope 2) are about 0.866-0.886 of those obtained with the stationary assumption. Moreover, the nonstationary responses to ground excitation of duration $T=10$ sec are about 0.895-0.914 of those induced when $T=15$

sec. i.e the internal forces increase with the increase of earthquake duration.

Effect of Spatial Variation of Earthquake Waves

The degree of cross correlation between multiple-support motions is specified by the parameter C in Eq.13. Figure (6) shows the variations of r.m.s internal forces with C. It can be observed that, the internal forces increase with C up to certain values then remain constant or slightly decrease. As C tends to 0 (the excitations become fully correlated) the internal forces decrease rapidly. Accordingly, the assumption of full correlation of motions at supports would result in zero differential motion between the bridge supports and a force-free rigid body motion. This would contradict the observations from previous earthquakes, in which most damage in bridges was attributed to both axial forces and bending moments. Therefore, it is important to consider the spatial variation of ground motion in the design and safety evaluation of multi-span bridges.

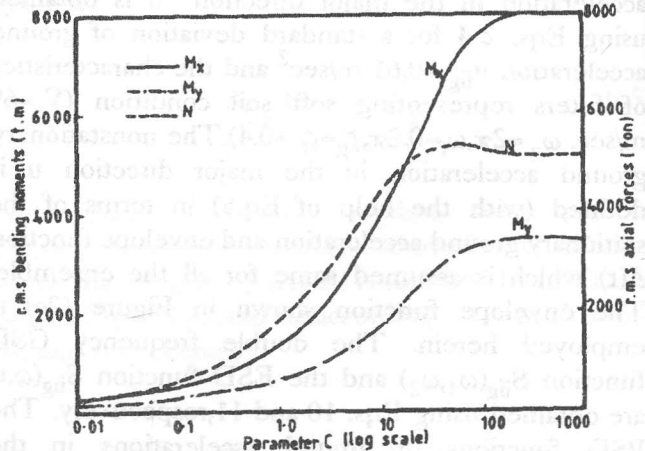


Figure 6. Variation of r.m.s internal forces with parameter C.

Effect of Angle of Incidence γ of Earthquake Waves

For different angles of incidence γ the r.m.s values of bending moments and axial forces at the interior supports are calculated and plotted versus γ in Figure (7). It can be noted that these forces reach their maximum values for $\gamma = 0$, i.e when the bridge is oriented in the direction of expected epicentre (direction of wave propagation).

Table 2. Stationary and nonstationary mean peak values of internal forces.

type of response	bending moment M_x			bending moment M_y			axial force N		
	r.m.s value	peak fac.	mean peak	r.m.s value	peak fac.	mean peak	r.m.s value	peak fac.	mean peak
nonstationary (envelope 1)	1059	1.694	1794	462	1.705	788	1459	1.677	2447
nonstationary (envelope 2)	1061	1.849	1962	464	1.896	880	1462	1.828	2673
stationary	1064	2.104	2239	467	2.176	1016	1466	2.058	3017

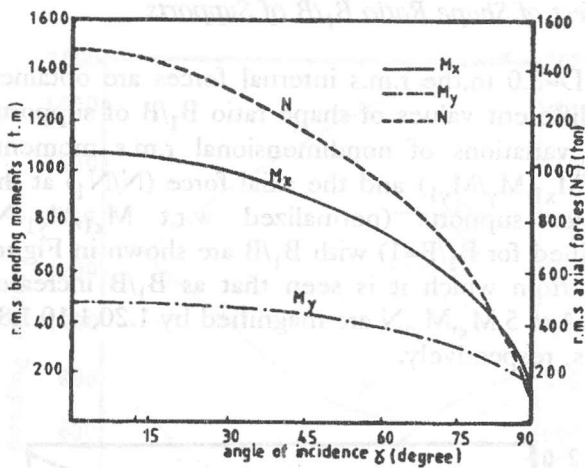


Figure 7. r.m.s internal forces VS angle of incidence γ .

As γ tends to 90, the excitations become fully correlated, the rigid body motion predominates, and the internal forces decrease considerably. For $\gamma=90^\circ$, M_x , M_y , N are reduced to 0.32, 0.61, 0.07 times those obtained when $\gamma=0$, respectively.

Effect of Soil-Support Interaction

The effect of soil-support interaction depends on the relative stiffness of the bridge-support system and the soil (represented by the shear wave velocity V_s). V_s is taken as variable parameter ranging between 30 m/sec (representing a very soft soil) and 630 m/sec (for soft rock providing almost a fixed-base condition) using a constant value of $C/V_s = 0.0091$ (to keep the same degree of

correlation) and utilizing the same acceleration spectra (corresponding to soft soil condition). The variation of r.m.s internal forces with V_s is shown in Figure (8). The interaction effect is pronounced for low values of V_s . As V_s increases, the internal forces increase, ultimately reaching their fixed-base condition (i.e no interaction effect takes place).

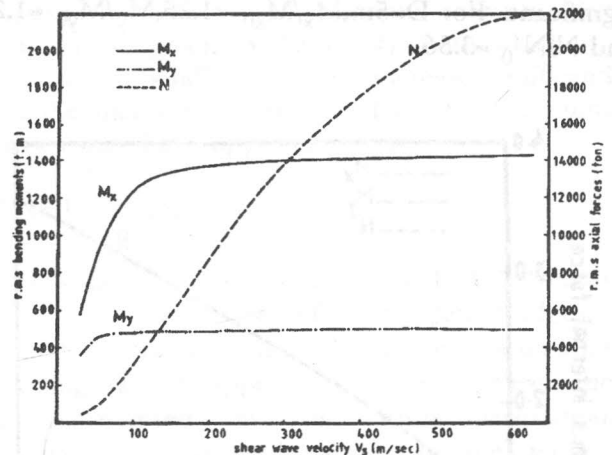


Figure 8. Variation of r.m.s internal forces with shear wave velocity.

It should be noted that, when the ground acceleration spectra are modified to account for the variation of dynamic characteristics $\omega_g, \zeta_g, \omega_f, \zeta_f$ of soil type, contrary results are observed as shown in Table (3), where the bending moments decrease sharply with the increase of V_s , while the axial forces increase up to $V_s = 330$ m/sec, then they decrease for any further increase of V_s .

Table 3. Effect of type of soil filter and associated ground spectrum.

type of soil filter	dynamic characteristics of soil filter			spectrum	r.m.s internal forces		
	V_s m/s	$\omega_g = 10 \omega_f$	$\xi_g = \xi_f$		M_x :(t.m)	M_y :(t.m)	N :(ton)
very soft	30	3.14	0.3	1	2363	1441	1256
soft	69	6.28	0.4	2	1064	467	1466
average	150	10.99	0.5	3	540	198	2296
firm	330	15.70	0.6	4	300	108	3170
extremely firm	550	31.40	0.8	5	93	35	1349
soft rock	630	47.10	0.9	6	49	19	755

Effect of Embedment Depth of Supports

Figure (9) shows the variations of nondimensional r.m.s moments $M_x/M_{x0}, M_y/M_{y0}$ and axial force N/N_0 at the interior supports (normalized w.r.t the M_{x0}, M_{y0}, N_0 obtained for surface supports) with the embedment depth D . The internal forces increase with the increase of D ; the increase of N is significant. For $D=5m, M_x/M_{x0} = 1.25, M_y/M_{y0} = 1.20$ and $N/N_0 = 3.56$.

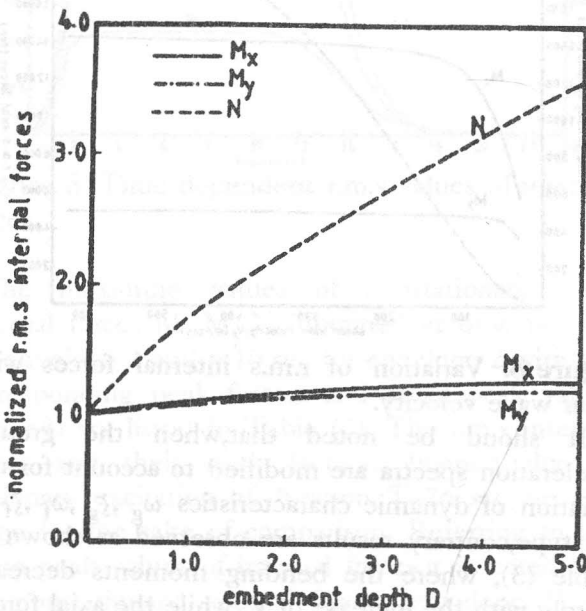


Figure 9. Variation of r.m.s internal forces with the embedment depth.

Effect of Shape Ratio B_1/B of Supports

For $D=2.0$ m, the r.m.s internal forces are obtained for different values of shape ratio B_1/B of supports. The variations of nondimensional r.m.s moments ($M_x/M_{x1}, M_y/M_{y1}$) and the axial force (N/N_1) at the interior supports (normalized w.r.t M_{x1}, M_{y1}, N_1 obtained for $B_1/B=1$) with B_1/B are shown in Figure (10), from which it is seen that as B_1/B increases from 1 to 5, M_x, M_y, N are magnified by 1.20, 1.10, 1.88 times, respectively.

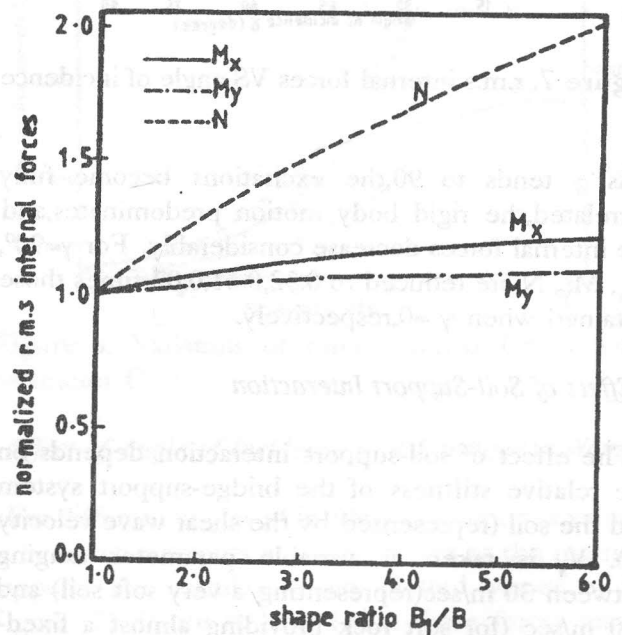


Figure 10. Variation of r.m.s internal forces with the support shape ratio.

Effect of Bridge Length L

For bridges having different lengths and same cross sectional area ($A=4.8m^2$, $I_x=3.6m^4$, $I_y=1.024m^4$), the r.m.s internal forces at the interior supports are obtained and plotted against the bridge length L in Figure (11). It is seen that the axial forces increase with L; but, the bending moments decrease with L up to certain values, then they increase. In this context, it should be mentioned that the increase of L implies two counteracting effects; (i) decrease of the degree of correlation which increases the internal forces, and (ii) decrease of bridge stiffness which reduces these forces.

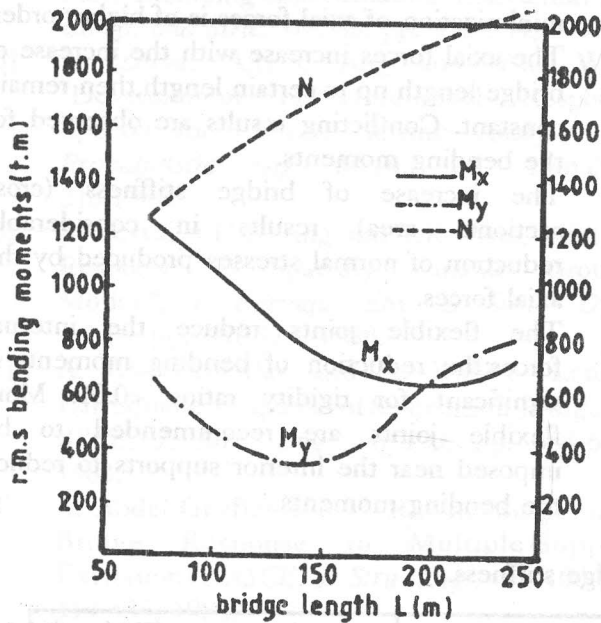


Figure 11. r.m. internal forces versus bridge length.

Effect of Flexibility of Expansion Joints

Figure (12) shows the variations of r.m.s internal forces at the interior supports with the rigidity ratios $r_x=(EI_x)_j/(EI_x)_b$, $r_y=(EI_y)_j/(EI_y)_b$, and $r_a=(EA)_j/(EA)_b$ of joint rigidity to bridge rigidity. From the figure, it is noted that, for rigidity ratios greater than 0.2, the effect of joints is marginal. Nevertheless, if $r_x=r_y=r_a=0.01$, considerable reductions (44%, 48%) of bending moments M_x, M_y are achieved.

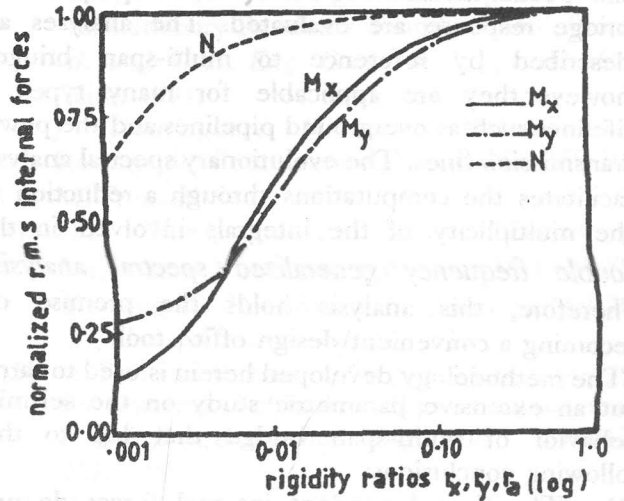


Figure 12. Effect of joint flexibility on the internal forces.

Effect of Bridge Stiffness

Different bridges having the same length $L=100m$ and variable cross sectional areas are analyzed. The properties of areas and the r.m.s internal forces obtained are given in Table (4), from which it is seen that the bending moments increase significantly with the increase of stiffness. However, the normal stresses may have opposite trends.

CONCLUSION

Stochastic methods are developed for evaluating the dynamic response of multi-span bridges to spatially variable multiple-support excitations including the soil-support interaction. The excitation are represented by the three translational components of earthquake ground motions acting in three mutually perpendicular directions and incident at an angle w.r.t a chosen set of global directions of the bridge. Each component is considered as stationary or nonstationary random process. The nonstationary process is expressed by the product of a stationary random process with a deterministic envelope function of arbitrary shape. Empirical formulas are employed for expressing the frequency-dependent impedance functions of soil. Spectral analyses are conducted to obtain the spectral density matrices (for stationary excitation) or the covariance matrices (for nonstationary excitations), from which

the spectral moments and the statistical properties of bridge response are evaluated. The analyses are described by reference to multi-span bridges; however, they are applicable for many types of lifelines, such as overground pipelines, and the power transmission lines. The evolutionary spectral analysis facilitates the computations through a reduction in the multiplicity of the integrals involved in the double frequency generalized spectral analysis. Therefore, this analysis holds the promise of becoming a convenient design office tool.

The methodology developed herein is used to carry out an extensive parametric study on the seismic behavior of multi-span bridge that led to the following conclusions:

- (1) The time-dependent internal forces do not overshoot the corresponding stationary internal forces. The ratios between the nonstationary and stationary mean peak values increase with the increase of earthquake duration; but, they are always less than unity.
- (2) The partially correlated support motions excite all modes and can give high differential displacements and result in significant internal forces. This agrees with the observed seismic damages of bridge in the past earthquakes. The assumption of fully correlated seismic inputs significantly underestimates the internal forces (especially the axial forces). Therefore, the spatial variation of seismic

excitation is of major importance and has to be considered in the design of multi-span bridges.

- (3) If the bridge is oriented perpendicular to the expected direction of epicentre, the excitation becomes fully correlated and the internal forces would be minimum. Maximum internal forces are induced in the bridge sections when the earthquake waves propagate in the direction of the longitudinal axis of bridge.
- (4) When the soil-support interaction is taken into account, the internal forces are decreased. The reduction is pronounced for softer soil and may lead to a significant saving of design cost.
- (5) The internal forces are minimized for surface supports (i.e. those having zero embedment depth) and square supports ($B_1/B=1.0$). The minimization of axial forces is of higher order.
- (6) The axial forces increase with the increase of bridge length up to certain length, then remain constant. Conflicting results are observed for the bending moments.
- (7) The increase of bridge stiffness (cross sectional area) results in considerable reduction of normal stresses produced by the axial forces.
- (8) The flexible joints reduce the internal forces; the reduction of bending moments is significant for rigidity ratios <0.01 . More flexible joints are recommended to be imposed near the interior supports to reduce the bending moments.

Table 4. Effect of bridge stiffness.

properties of areas			internal forces			normal stresses : (Kg/cm ²)		
A : (m ²)	I _x : (m ⁴)	I _y : (m ⁴)	M _x : (t.m)	M _y : (t.m)	N : (ton)	f _{Mx}	f _{My}	f _N
0.66	0.066	0.020	33	16	1078	27.5	24.0	163.3
1.20	0.225	0.064	90	40	1250	30.0	25.0	104.2
2.64	1.065	0.317	390	153	1400	40.3	29.0	53.0
4.80	3.600	1.024	1064	467	1466	44.3	36.5	30.5
7.40	8.442	2.467	1890	996	1497	41.4	40.4	20.2
10.56	17.037	5.069	2789	1714	1515	36.0	40.6	14.3

REFERENCES

- [1] I. Nelson and P. Weidlinger "Dynamic Seismic Analysis of Long Segmented Lifelines", *ASME, J. Press. Ves. Tech.*, vol. 101, pp. 10-20, 1979.
- [2] D. Somaini, "Seismic Behaviour of Girder Bridges for Horizontally propagating Waves", *J. Earthqu. Eng. & Struc. Dyn.* vol. 15, pp. 777-793, 1987.
- [3] A. Nazmy and A. Abdel-Ghaffar, "Non-Linear Earthquake Response Analysis of Long-Span Cable-Stayed Bridges", *J. Earthqu. Eng. & Struc. Dyn.*, vol. 19, pp. 45-76, 1990.
- [4] C. Spyrcos, "Seismic Behaviour of Bridge Piers Including Soil-Structure Interaction", *J. Comp. and Struc.*, vol. 43, pp. 373-384, 1992.
- [5] A. Zerva, A.H-S. Ang and Y.K. Wen, "Development of Differential Response Spectra for Lifeline Seismic Analysis", *J. Probabilistic Eng. Mech.*, vol. 1, pp. 208-218, 1986.
- [6] A. Zerva, A.H-S. Ang and Y.K. Wen, "Lifeline Response to Spatially Variable Ground Motion", *J. Earthqu. Eng. & Struc. Dyn.*, vol. 16, pp. 361-379, 1988.
- [7] A. Abdel-Ghaffar and L. Rubin, "Lateral Earthquake Response of Suspension Bridges.", *ASCE, J. Struc. Eng.*, vol. 109, pp. 664-675, 1983.
- [8] A. Abdel-Ghaffar and L. Rubin, "Suspension Bridge Response to Multiple-Support Excitations", *ASCE, J. Struc. Eng.*, vol. 108 pp. 419-435, 1982.
- [9] M.C. Lee and J. Penzien, "Stochastic Analysis of Structures and Piping Systems Subjected to Stationary Multiple Support Excitations", *J. Earthqu. Eng. & Struc. Dyn.*, vol. 11, pp. 91-110, 1983.
- [10] E. Zavoni and E. Vanmarcke "Seismic Random Vibration Analysis of Multisupport Structural Systems", *ASCE, J. Eng. Mech.*, vol. 120, pp. 1107-1128, 1994.
- [11] H. Soliman and T.K. Datta, "Response of Multi-Span Bridges to Random Ground Motion", *Proc. Int. Conf. on New Dimensions on Bridges and Flyovers*, Singapore. June 1991
- [12] E.A. Mashaly, "Evolutionary Response Analysis of Underground Pipelines to Nonstationary Random Ground Motion", *Proc. 4th Arab Struc. Eng. Conf.* vol. 3, pp. 343-360, Cairo, 1991.
- [13] J. Dominguez, "Dynamic Stiffness of Rectangular Foundations", *Report*, No. R78-20, MIT, Cambridge, 1978.
- [14] H.L. Wong and J.E. Luco, "Tables of Impedance Functions and Input Motions for Rectangular Foundations", *Report* No. CE78-15, Univ. of Southern Calif., 1978.
- [15] A. Pais and E. Kausel, "Approximate Formulas for Dynamic Stiffness of Rigid Foundations", *J. Soil Dyn. & Earthqu. Eng.*, vol. 7, pp. 213-227, 1988.
- [16] R.W. Clough and J. Penzien, *Dynamics of Structures*, Mc.Graw Hill, 1982
- [17] J.S. Bendat and A.G. Piersol, *Random Data*, John Wiley & Sons, 1986.
- [18] M.B. Priestley, "Power Spectral Analysis of Nonstationary Random Processes", *J. Sound Vib.*, vol. 6, pp. 86-97, 1967.
- [19] A. Hindi and M. Novak, "Pipeline Response to Random Ground Motion", *ASCE, J. Eng. Mech.*, vol. 106, pp. 339-360, 1980.
- [20] R. Harichandran and E. Vanmarcke, "Stochastic Variation of Earthquake Ground Motion in Space and Time", *ASCE, J. Eng. Mech.*, vol. 112, pp. 154-174, 1986.
- [21] C-H. Loh, "Analysis of the Spatial Variation of Seismic Waves and Ground Movements from SMART-1 Array Data", *J. Earthqu. Eng. & Struc. Dyn.* vol. 13, pp. 561-581, 1985.
- [22] A.F. Abdel-Rahman and E.A. Mashaly "Seismic Response of Buried Jointed Pipelines", *Proc., 1st Alex. Conf. Struc. & Geotec. Eng.* pp. 303-317, 1990.
- [23] E.A. Mashaly, "Response of Jointed Concrete Dams to Nonstationary Random Ground Motion", *Proc. Al-Azhar Eng. 4th. Int. Conf.*, vol. 3 pp. 201-216, 1995.
- [24] N.C. Nigam, *Introduction to Random Vibrations*, The MIT Press. Cambridge, Massachusetts, London, England, 1983.
- [25] A.G. Davenport, "Note on the Distribution of the Largest Value of Random Function with Application to Gust Loading", *Proc. Inst. Civil Engrs.*, vol. 28, pp. 187-196, 1963.